Proceedings of the 3rd International Conference on Control, Dynamic Systems, and Robotics (CDSR'16)
Ottawa, Canada - May 9 - 10, 2016
Paper No. 102
DOI: 10.11159/cdsr16.102

Modeling and Motion Control of a Magnetically Navigated Microrobotic System

Xiaodong Zhang, Mir Behrad Khamesee
Department of Mechanical and Mechatronics Engineering/University of Waterloo
200 University Ave West, Waterloo, Canada
x442zhan@uwaterloo.ca; khamesee@uwaterloo.ca

Abstract - This paper presents a technology for remotely navigating a magnetized microrobot in three-degree-of-freedom (3-DOF) using magnetic energy. The magnetic energy source is a magnetic drive unit that consists of six iron-core electromagnets, a soft-iron yoke, and a soft-iron pole-piece. The dynamic models of the magnetically navigated microrobot were derived from the magnetic field model in the workspace. An experimental method was applied to define the magnetic field model. Based on the derived dynamic models, a feed-forward plus standard PID controller was used to control the motion of the microrobot with 3-DOF. Experiment was conducted to validate the performance of the proposed controller. The experimental results showed $20\mu m$ motion accuracy in 3-DOF in a motion range of $10 \times 10 \times 30 mm^3$.

Keywords: Magnetic navigation, Microrobot, Magnetic field, PID plus feedforward controller

1. Introduction

Micromanipulation involves performing tasks using macro scale end-effectors that have micro motion accuracy, and using micro scale end-effectors directly. For the first case, the end-effector of a micromanipulator has a mechanical arm connecting it to its base. This type of micromanipulator includes lead-screw driving stages and piezoelectric actuators [1, 2, 3]. However, the mechanical connection produces frictions, vibration, and backlash that degrade the performance of micromanipulation. For the second case, an end-effector is remotely manipulated without any mechanical connection to the base of a micromanipulator. This type of micromanipulator is capable of working in hazard and out-of-reach environments. Magnetic levitation micromanipulators, having remotely manipulated micro end-effector and micrometer motion accuracy, are most frequently studied and have promising potential in biomedical applications [4, 5, 6, 7, 8].

Active magnetic navigation of a microrobot requires a controlled magnetic field source. Generally, electromagnets are used for multi-dimensional manipulation of a microrobot [9, 10, 11, 12]. The magnetic field generated by electromagnets is controlled by a current. The multi-degree of motion freedom of a robot is achieved by setting up special configurations of multi-electromagnets. Since the strength of the magnetic field decays rapidly as the distance from electromagnet increases, an iron-core is commonly used to significantly enhance the magnetic field strength outside the electromagnet. This enhanced magnetic field can then expand the workspace of the microrobot.

Modeling the magnetic field in the microrobots workspace is crucial to developing a magnetic navigation system. For systems that have air-core coils and permanent magnets produced magnetic field, analytical methods such as Bio-Savart Law and Amperes Law are applied to find a closed-form magnetic field model. However, for systems that have iron-core electromagnets produced magnetic field, the iron results in high nonlinearity in the whole system. Therefore, it is difficult to find a closed-form for modeling the magnetic field in the workspace. Alternative solutions are numerical and experimental methods which uses simulation and measurement data to find a fitting model that match the real magnetic field with minimum error.

Another important aspect of studying a magnetic navigation system has been focused on development of controllers for active and precise navigation of a microrobot. These control mechanisms include but not limit to sliding-mode control [13], feedback linearization [14], fuzzy logic [15], and neural network [16]. In [14], a state feedback controller was proposed to navigate a small magnetized robot in the vertical direction with 16m accuracy. Lin in [17] proposed using a combination of traditional sliding-mode control system and a radial basis function network estimator for positioning the levitated object of a magnetic levitation system. The sliding-mode controller was used to provide basic levitation of the object. The estimator was then implemented to improve the robustness of levitation.Khamesee in [18] compared the performance of a standard PID and adaptive controllers on a magnetic levitation stage. It was indicated that the performance of navigation could be improved by choosing advanced controllers.

This paper is organized as follows: Section 2 introduces the configuration of the magnetic levitation system. Section 3 presents the modeling of the magnetic field in the workspace of the microrobot. The controller design is presented in Section 4. Then the experimental results will be shown in Section 5. Section 6 briefly summarizes the work in this paper.

2. Configuration of the Magnetic Levitation System

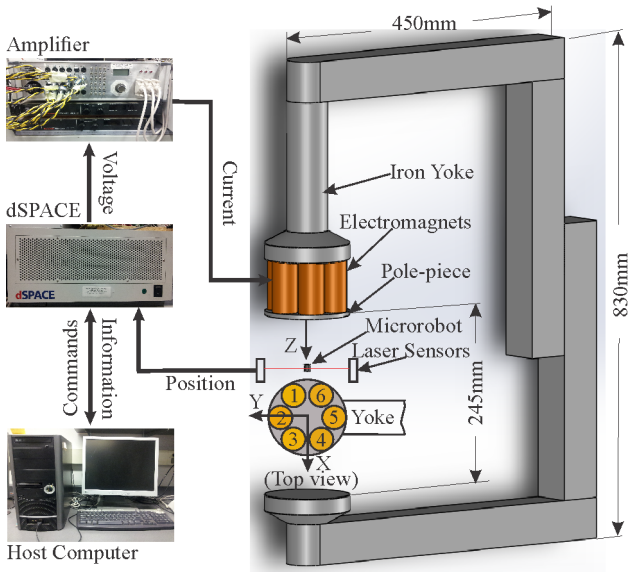

Fig. 1: The configuration of the magnetic levitation system.

The magnetic levitation system was previously developed in the Maglev Microroboticlab, at the University of Waterloo. Its configuration is shown in Fig. 1. The system consists of a magnetic drive unit, laser sensor position detection system, a dSPACE controller, a host computer, and an amplifier as current output unit.The magnetic drive unit (MDU) is used to generate the source magnetic field for levitating a magnetized object. It is composed of soft iron yoke, six pairs of iron-core electromagnets,and a soft iron pole-piece. The pole-piece connects the electromagnets, and forms the desired magnetic field in the workspace. The relatively permeability r of the yoke andthe pole-piece is 4000. All electromagnets have a configuration of 840 turns, 20mm outer radius, 10mm inner radius, and 40mm length. A dSPACE real-time controller functions as the central control unit of the whole system. It has ControlDesk user interface, and is able to compile directly in Simulink software environment. The laser sensor used for position detection is LS-5041 from KEYENCE Company. Three sets of laser sensor, installed surrounding the workspace, are used to measure the three dimensional position of the levitated microrobot.

3. System Modeling

3.1. Modeling the Magnetic Field in the Workspace

In a contact-free levitation, a magnetic levitation system generates satisfied levitation force to compensate the gravity force on a magnetized object, and to maintain a desired dynamics of the object. A small object that is evenly magnetized with a total magnetization M is placed in an external magnetic field, the total force on the magnetized object is:

$$F = \nabla(\vec{M} \cdot \vec{B}) \tag{1}$$

where, $\vec{B}$ is the magnetic flux density in the workspace where the object stays. In this study, the magnetization direction of the object is supposed to be aligned in the z-direction, i.e., $\vec{M} = [0,0,M_0]$. Therefore, the magnetic forces are related to the gradient of the vertical direction magnetic field$[\frac{dB_z}{dx}, \frac{dB_z}{dy}, \frac{dB_z}{dz}]$.

For the developed magnetic levitation system, it is impossible to find a closed form for modeling the magnetic field in the air-gap, because the soft-iron yoke, iron-core electromagnets, and pole-piece simply result in high nonlinearity in the whole system. Therefore, experimental method is applied. A Hall-effect sensor was used to scan the workspace and to record the magnetic flux density in real time. Fig. 2 is the magnetic flux density measured at 75mm below the pole-piece while electromagnet 1 was powered with one Ampere current.

The magnetic field produced by one electromagnet is linear to the current in this electromagnet. According to the measured data presented in Fig. 2, the magnetic field produced by electromagnet 1 can be modeled as:

$$B_{z1} = (a_{1x}x^2 + b_{1x}x + c_{1x})I_1 \tag{2}$$

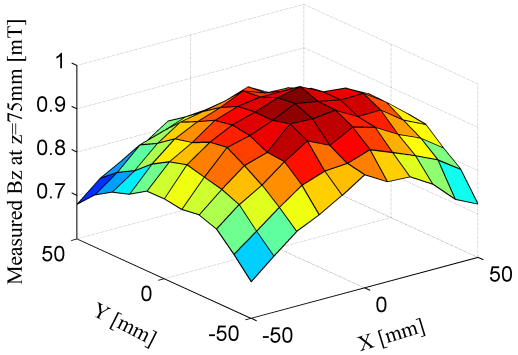

Fig. 2: Magnetic flux density measured at 75mm below the pole-piece while electromagnet 1 is powered with one Ampere current.

where, a_{1x} is a function of the z. b_{1x} and c_{1x} are functions of z and y. I_1 is the current in electromagnet 1.

The magnetic flux density produced by other electromagnets can be modeled in the same way. The total magnetic flux density in the workspace is the linear summation of magnetic flux density produced by all electromagnets:

$$B_z = \sum_{i=1}^{6} B_{zi} \tag{3}$$

By considering the geometric symmetry, the total magnetic flux density can be expressed as:

$$\begin{aligned} B_z = (a_{1x}x^2 + b_{1x}x + c_{1x})I_1 + (a_{2x}x^2 + c_{2x})I_2 \\ +(a_{1x}x^2 - b_{1x}x + c_{1x})I_3 + (a_{4x}x^2 + b_{4x}x + c_{4x})I_4 \\ +(a_{5x}x^2 + c_{5x})I_5 + (a_{4x}x^2 - b_{4x}x + c_{4x})I_6 \end{aligned} \tag{4}$$

where, a_{2x}, a_{4x} and a_{5x} are functions of z. b_{4x}, c_{2x}, c_{cx}, and c_{5x} are functions of z and y. $I_i (i = 1, ..., 6)$ are the current in the number i electromagnet.

3.2. Dynamic Modeling

Substitute equation 4 into the force mode represented by equation 1, and linearize at the center $[0, 0, z_0, I_0]$ of the workspace, The magnetic forces on a magnetized object with volume magnetization M are expressed as:

$$F_x = M\frac{\partial B_z}{\partial x} = 2xI_0\,(a_{x1}z_0 + b_{x1}) + (a_{x2}z_0 + b_{x2})\,(i_1 - i_3 + i_4 - i_6) \tag{5}$$

$$F_y = M\frac{\partial B_z}{\partial y} = 2yI_0\,(a_{y1}z_0 + b_{y1}) + (a_{y2}z_0 + b_{y2})\,(i_1 + 2i_2 + i_3 - i_4 - 2i_5 - i_6) \tag{6}$$

$$F_z = M\frac{\partial B_z}{\partial z} = (a_z z + b_z)\,I_0 + a_z I_0\,(z - z_0) + (a_z z_0 + b_z)\,(i_i + i_2 + i_3 + i_4 + i_5 + i_6) \tag{7}$$

where I_0 is the current in electromagnets when the levitated robot stays at z_0. All coefficients in equations 5-7 are deduced from coefficients in equation 4. $i_j, j = 1, , 6$ are the perturbed current in the jth electromagnet.

In a contact free levitation state, the dynamic of the levitated object is obtained using the Newtons Second Law:

$$m\ddot{x} = 2xI_0\,(a_{x1}z_0 + b_{x1}) + (a_{x2}z_0 + b_{x2})\underbrace{(i_1 - i_3 + i_4 - i_6)}_{u_x} \tag{8}$$

$$m\ddot{y} = 2yI_0\,(a_{y1}z_0 + b_{y1}) + (a_{y2}z_0 + b_{y2})\underbrace{(i_1 + 2i_2 + i_3 - i_4 - 2i_5 - i_6)}_{u_y} \tag{9}$$

$$m\ddot{z} = -a_z I_0\,(z - z_0) + (a_z z_0 + b_z)\underbrace{(i_i + i_2 + i_3 + i_4 + i_5 + i_6)}_{u_z} \tag{10}$$

where, m is the total mass of the microrobot.

3.3. PID Control

The levitation in horizontal directions is internally stable. However, the levitation in vertical direction is internally unstable due to the gravity force. Therefore, feedback control is necessary for a stable levitation. Using the derived dynamics model, a PID plus feed forward controller is proposed to control the three-dimensional motion of a small permanent magnet in a contact free space. The schematic of the controller is shown in Fig. 3. In the vertical direction levitation, the feed forward controller provides the major control signal that compensates the gravity force at steady state:

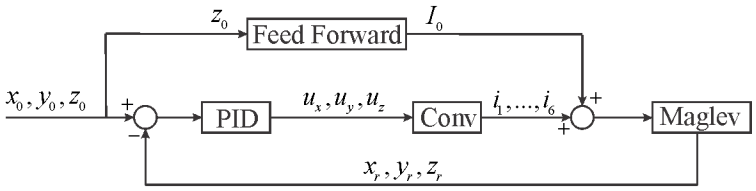

Fig. 3: Schematic of the PID plus feed forward controller for three-dimensional motion control.

$$I_0 = \frac{mg}{2a_z z - a_z z_0 + b_z} \tag{11}$$

The PID controller is used to compensate for the actual signal. Three virtual control inputs u_x, u_y, u_z are calculated from the PID control law:

$$u_{(x,y,z)}(t) = K_p e_{(x,y,z)}(t) + K_I \int e_{(x,y,z)}(t) + K_D \dot{e}_{(x,y,z)}(t) \tag{12}$$

where e_x, e_y, e_z are the error between the reference and the real positions of the microrobot in three axis.

The virtual control inputs are then converted to actual current input to electromagnets using the pseudo inverse method, which minimizes the normal of input signal.

$$\begin{bmatrix} i_1 \\ i_2 \\ i_3 \\ i_4 \\ i_5 \\ i_6 \end{bmatrix} = \underbrace{\begin{bmatrix} 0.25 & 0.0833 & 0.1667 \\ 0 & 0.1667 & 0.1667 \\ -0.25 & 0.0833 & 0.1667 \\ 0.25 & -0.0833 & 0.1667 \\ 0 & -0.1667 & 0.1667 \\ -0.25 & -0.0833 & 0.1667 \end{bmatrix}}_{\textbf{Conv}} \begin{bmatrix} u_x \\ u_y \\ u_z \end{bmatrix} \tag{13}$$

4. Experiment and Results

Three-dimensional motion control experiment was conducted to validate the performance of the proposed controller. In the experiment, the levitated microrobot is a small cylindrical permanent magnet that has 5mm in diameter and 5mm in height. The mass of the microrobot is 0.83g. It has a remnant magnetic flux density of 0.29T. The configuration of the levitated microrobot is shown in Fig. 4. The parameters of the PID controllers in three axis are shown in Table 1

Table 1: Parameters of PID controllers.

Controller	K_P	K_I	K_D
PID-x	1000	1500	0.1
PID-x	1000	1500	0.1
PID-x	4500	2000	30

The step motion response in three directions was recorded in the experiment. The experimental results are presented in Fig. 5. The experimental performance shows that the proposed PID plus feed forward controller can provide $20\mu m$ motion accuracy in three axes in a working volume of 10mm × 10mm × 30mm. The working volume is limited by the dimension of the levition robot, as well as the configuration of the magnetic drive unit. The levitation in the vertical direction is internally unstable. Therefore, levitation in this direction is sensitive to the environment noise and power supply quality. The overshoot of the step response in the vertical direction can be smoothed by adding damping element to the robot. It should be noted that cross-coupling effect exists among three motion axes. The motion in y direction has a significant impact on the stable levitation of the other two directions. In order to reduce the cross-coupling effect, advanced controller, such as LQG controller, can be implemented to control the motion of the microrobot.

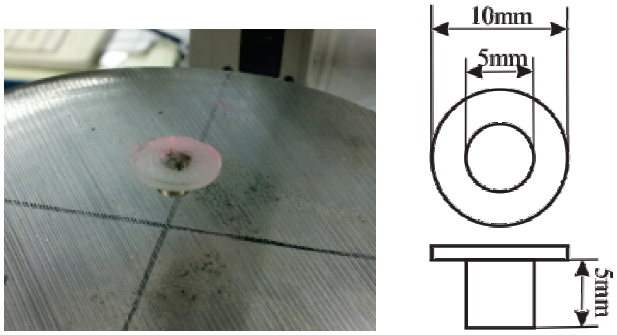

Fig. 4: Configuration of levitated microrobot.

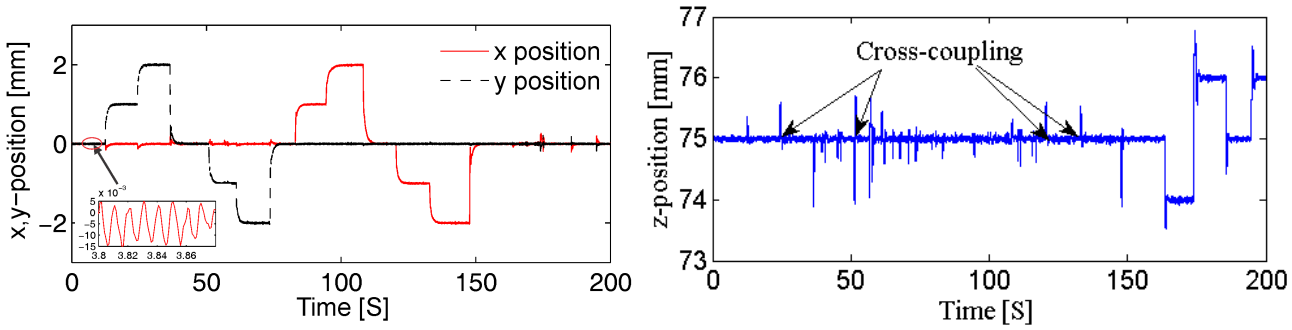

Fig. 5: Three-dimensional step-response motion control of the microrobot.

5. Conclusion

This paper presented the modeling and control of a magnetically navigated micromanipulator. The magnetic field model in the workspace was developed using the experimental method. The dynamic models of the microrobot show high nonlinearity. The acquired models were linearized to develop PID controller for the three-dimensional motion control of the microrobot. The PID controllers show acceptable performance in navigation in a motion range of $10 \times 10 \times 30 mm^3$.

In the experiment, it was noted that cross-coupling effect existed. This reduced the positioning accuracy, and degraded the stability of navigation. A future work could be involved in the development of advanced controller to reduce the cross-coupling effect.

References

[1] J. Liu, et al, "Automated vitrification of embryos," *IEEE Robotics and Automation Magazine*, 2015.

[2] F. Karimirad, B. Shirinzadeh, W. Yan ,"A vision-based methodology to dynamically track and describe cell deformation during cell micromanipulation," *Internation Journal of Optomechatronics*, vol. 7, no. 1, pp. 33-45, 2013.

[3] E. Avci, et al, "Toward high-speed automated micromanipulation," *IEEE International Conference on Robotics and Automation*, Karlsruhe, Germany, 2013, pp.1718-1723.

[4] M. Mehrtash, N. Tsuda, M.B. Khamesee, "Bilateral macro-micro teleoperation using magnetic levitation," *IEEE/ASME Transactions on Mechatronics*, vol. 16, no. 3, pp.459-469, 2011.

[5] K. Peyer, L. Zhang, B. J. Nelson, "Bio-inspired magnetic swimming microrobots for biomedical applications," *Nanoscale*, vol. 5, pp. 1259-1272, 2013.

[6] S. Martel, et al, "Flagellated magnetotactic bacteria as controlled MRI-trackable propulsion and steering systems for medical nanorobots operating in the human microvasculature," *The International Journal of Robotic Research*, vol.28, no. 4, pp.571-582, 2009.

[7] M. S. Grady, et al, "Nonlinear magnetic stereotaxis: three-dimensional in vivo remote magnetic manipulation of a small object in canine brain," *Medical Physics*, vol. 17, no. 3, pp.405-415, 1990.

[8] F. Carpi, C. Pappone, "Magnetic maneuvering of endoscopic capsules by means of a robotic navigation system," *IEEE Transactions on Biomedical Engineering*, vol. 56, no. 5, pp.1482-1490, 2009.

[9] C. Elbuken, M. B. Khamesee, "Design and implementation of a micromanipulation system using a magnetically levitated MEMS robot," *IEEE/ASME Transactions on Mechatronics*, vol. 14, no. 4, pp. 434-445, 2009

[10] M. P. Kummer, et al, "OctoMag: an electromagnetic system for 5-DOF wireless micromanipulation," *IEEE Transactions on Robotics*, vol. 26, no. 6, pp.1006-1017, 2010.
[11] E. B. Steager, et al, "Automated biomanipulation of single cells using magnetic microrobots," *International Journal of Robotic Research*, vol. 32, no. 3, pp.346-359, 2013.
[12] C. Gosse, V. Croquette, "Magnetic tweezers: micromanipulation and force measurement at the molecular level," *Biophysical Journal*, vol. 82, pp.314-3329, 2002.
[13] B. M. Mustapha, J. D. Jiya, "Sliding mode control of a magnetic levitation system," International Journal of Engineering and Applied Sciences, vol. 6, no. 2, pp.14-17, 2014.
[14] E. Shameli, M. B. Khamesee, J. P. Huissoon, "Nonlinear controller design for a magnetic levitation device," Microsystem Technologies, vol. 13, no. 8, pp. 831-835, 2007.
[15] S. K. Hong, et al, "Robust fuzzy control of a magnetic bearing system subject to harmonic disturbance," IEEE Transactions on Control Systems Technology, vol. 8, no. 2, pp. 366-371, 2000.
[16] R. J. Wai, et al, "Adaptive fuzzy-neural-network control for maglev transportation system," IEEE Transactions on Neural Networks, vol. 19, no. 1, pp. 54-70, 2008.
[17] F. J. Lin, et al, "Intelligent sliding-mode control using RBFN for magnetic levitation system," IEEE Transactions on Industrial Electronics, vol. 54, no. 3, pp. 1752-1762, 2007.
[18] M. B. Khamesee, et al, "Design and control of a microrobotic system using magnetic levitation," IEEE/ASME Transactions on Mechatronics, vol. 7, no. 1, pp. 1-14, 2002.